

Molecular organization in self-assembled binary porphyrin nanotubes revealed by resonance Raman spectroscopy

Ricardo Franco,^{*a} John L. Jacobsen,^b Haorong Wang,^c Zhongchun Wang,^c Krisztina István,^a Neil E. Schore,^b Yujiang Song,^{†c} Craig J. Medforth^{cd} and John A. Shelnutt^{*ce}

Received 10th December 2009, Accepted 12th February 2010

First published as an Advance Article on the web 9th March 2010

DOI: 10.1039/b926068d

Porphyrin nanotubes were formed by the ionic self-assembly of tetrakis(4-sulfonatophenyl) porphyrin diacid ($\text{H}_4\text{TPPS}_4^{2-}$) and Sn(IV) tetra(4-pyridyl) porphyrin ($\text{Sn}(\text{OH}^-)(\text{X})\text{TPyP}^{4+/5+}$ [$\text{X} = \text{OH}^-$ or H_2O]) at pH 2.0. As reported previously, the tubes are hollow as revealed by transmission electron microscopy, approximately 60 nm in diameter, and can be up to several micrometres long. The absorption spectrum of the porphyrin nanotubes presents monomer-like Soret bands, as well as two additional red-shifted bands characteristic of porphyrin *J*-aggregates (offset face-to-face stacks). To elucidate the origin of the *J*-aggregate bands and the internal interactions of the porphyrins, the resonance Raman spectra have been obtained for the porphyrin nanotubes with excitations near resonance with the Soret *J*-aggregate band and the monomer-like bands. The resonance Raman data reveal that the Sn porphyrins are not electronically coupled to the *J*-aggregates within the tubes, which are formed exclusively by $\text{H}_4\text{TPPS}_4^{2-}$. This suggests that the internal structure of the nanotubes has $\text{H}_4\text{TPPS}_4^{2-}$ in aggregates that are similar to the widely studied $\text{H}_4\text{TPPS}_4^{2-}$ self-aggregates and that are segregated from the Sn porphyrins. Possible internal structures of the nanotubes and mechanisms for their formation are discussed.

I. Introduction

Self-assembled porphyrin nanostructures are of great interest because of their promise as catalysts and optoelectronic nanomaterials.^{1–8} Porphyrin nanostructures are particularly promising as light-harvesting⁹ and energy- and electron-transfer components of solar energy utilizing devices, as they have interesting supramolecular porphyrin structures and properties analogous to those displayed by porphyrin hetero-dyads¹⁰ and pentamers.¹¹ Self-assembled porphyrin nanostructures may also serve as illuminating models of biological light-harvesting structures like the bacteriochlorophyll nanorods of the chlorosomes of green bacteria.^{12,13} Well-defined nanostructures such as porphyrin nanorods,⁸ nanotubes,^{2,14} nanofibers,^{15,16} nanosheets,^{17,18} nanospheres,⁹ and other morphologies^{19–21} have recently been reported. The porphyrin nanotubes (PNTs) formed by ionic self-assembly of two porphyrins with opposite

charge are of particular interest because their hollow tubular structure lends itself to the construction of nanotube-metal composites of various architectures.²² The PNTs are representative of a new class of porphyrin nanostructures for which the molecular building blocks (tectons) can be altered to control their structural and functional properties.² However, to realize nanodevices based on these PNTs and related porphyrin nanostructures, the organization of the porphyrin molecules in the tubes needs to be understood and the collective electronic properties of the tubes determined. For nanostructures, often direct X-ray structural methods may not be successful and indirect techniques must be employed. Herein, we report a resonance Raman study of the porphyrin nanotubes that provides insights into the electronic coupling and the packing arrangement of the porphyrin subunits.

II. Experimental

A Synthesis of the porphyrin nanotubes

The nanotubes were synthesized using a procedure similar to that reported previously.² All solutions were prepared using HPLC grade water (Aldrich). Tetrakis(4-sulfonato-phenyl)-porphyrin (H_2TPPS_4) tetrasodium salt was purchased from Aldrich and Sn(IV) tetrakis(4-pyridyl)porphyrin (SnTPyP^{2+}) dichloride was purchased from Frontier Scientific. H_2TPPS_4 stock solution (98.7 μM) was prepared by dissolving 10.1 mg of H_2TPPS_4 in 100 mL of water. The stock solution was green with a pH of 5.5. SnTPyP dichloride stock solution (42.6 μM) was prepared by dissolving 8.6 mg of SnTPyP in 250 mL of

^a REQUIMTE, Departamento de Química, Faculdade de Ciências e Tecnologia, Universidade Nova de Lisboa, 2829-516 Caparica, Portugal. E-mail: r.franco@dq.fct.unl.pt; Tel: +251-21-294-9659

^b Department of Chemistry, University of California, Davis, CA 95616, USA

^c Advanced Materials Laboratory, Sandia National Laboratories, 1001 University Blvd SE, Albuquerque, NM 87185-1349, USA. E-mail: jasheln@umm.edu; Fax: +1 505-272-7077; Tel: +1 505-272-7160

^d Department of Chemical and Nuclear Engineering, University of New Mexico, Albuquerque, NM 87106, USA

^e Department of Chemistry, University of Georgia, Athens, GA 30602, USA

[†] Present address: Dalian Institute of Chemical Physics, Chinese Academy of Sciences, Dalian, Liaoning, China

water. This stock solution was magenta pink and had a pH of 4.5. Small volumes (1–6 mL) of the stock solutions were filtered immediately prior to their use in the self-assembly reactions (Kendall monoject™ Tuberculin 1 mL syringes were used to pass the solutions through Pall Life Sciences Acrodisc® 13 mm syringe filters with 0.2 µm Supor® membranes).

Self-assembly experiments were conducted in 20 mL glass vials that had been rinsed with HPLC grade water. SnTPyP solution (3.5 µM) was prepared by diluting 739 µL of stock solution to a volume of 9 mL, followed by thorough mixing. A 10.5 µM solution of H₄TPPS₄ was prepared in a separate vial; 7.863 mL of water was added to 957 µL of H₂TPPS₄ stock solution, 180 µL of 1 M HCl was added, and the solution thoroughly mixed. The diluted and acidified solutions of H₂TPPS₄ were green consistent with the formation of the diacid species expected at this pH.

The SnTPyP solution was then added to the H₄TPPS₄ solution and the mixture thoroughly homogenized, producing a yellowish-green solution with H₄TPPS₄, SnTPyP and HCl concentrations of 5.25 µM, 1.75 µM, and 10 mM. The pH was carefully adjusted to 2.0 ± 0.1 using 1 M HCl. The vial was sealed and the solution left undisturbed in the dark for 72 h, after which time samples were taken for TEM, UV-visible absorption, and resonance Raman experiments as described below.

B Structural characterization

To prepare the TEM samples, ~5 µL of solution containing precipitate were removed from the bottom of the vial, followed by the removal of ~5 µL of the supernatant into the same pipette tip. This 10 µL aliquot was dispensed onto a standard holey carbon-coated copper TEM grid resting on a Kimwipe; the Kimwipe wicked away excess water. Transmission electron microscopy images of the samples were obtained using a 200 keV JEOL 2010 microscope.

C UV-visible spectroscopy

UV-visible spectra of the constituent porphyrins and the porphyrin nanotubes were obtained with a Hewlett Packard 8452A diode array spectrometer. Samples of the individual porphyrins were prepared by dilution of the previously prepared stock solutions to 10 µM with 0.01 M HCl (final pH of 2). UV-visible absorption spectra were obtained on the freshly prepared samples.

After centrifugation, samples of the porphyrin nanotubes were extracted from the precipitate rich layer at the bottom of the vial in which the nanotubes were synthesized (see Section A). Samples were transferred to a quartz cell with a beam path length of 1 cm, and UV-visible spectra were obtained and plotted using SigmaPlot (SPSS).

D Resonance Raman spectroscopy

Samples of the individual porphyrins were prepared at 100 µM concentrations in 0.01 M HCl. Samples of the porphyrin nanotubes were prepared by centrifuging the nanotube solution described in Section A and re-suspending the precipitate in 0.01 M HCl to produce a 10 times more concentrated suspension. The Raman samples, in a final volume of ~100 µL,

were transferred into a stoppered 3 × 3 mm cross-section optical cell (NSG Precision Cells). Typically, the spectra were taken at room temperature (24 °C) with data collection times of 2–10 min using a laser beam power of 20 mW.

The spectra were obtained using the 413.1 and 406.7 nm lines of an INNOVA 302 Kr⁺ laser (Coherent) or using the 496.5 and 501.7 nm lines of an INNOVA 304 Ar⁺ laser (Coherent). The Raman spectrometer was a 0.75 m monochromator (Instruments, SA) with a 512 × 2048 pixel LN₂-cooled CCD detector. The slit width of 100 µm for the 2400 groove mm⁻¹ holographic grating gives a spectral resolution of 2 cm⁻¹. The CCD array was cooled to 138 K by liquid nitrogen and controlled by a Symphony (Horiba Jobin Yvon) CCD controller unit. The columns of the CCD chip (EEV) were binned to give 2048 13.5 µm channels or 0.3 cm⁻¹ per channel. The chip is back-illuminated and has visible-NIR antireflection coatings. The spectrometer was interfaced to a personal computer *via* an IEEE 488.2 PCI-GPIB interface card (National Instruments), and LabSpec Raman Spectroscopy Software (Horiba JobinYvon) was used to control the spectrometer. Position mode was used for CCD detection covering about 500 cm⁻¹ of the Raman spectrum. Spectra were exported as even-X ASCII files for plotting with SigmaPlot (SPSS). Presented resonance Raman spectra were obtained for the 1300–1700 cm⁻¹ wavenumber range. Lower frequency spectra were not useful due to the intense resonance light scattering of the nanotube samples for wavenumbers below *ca.* 1000 cm⁻¹.

III. Results

A Porphyrin nanotubes

Porphyrin nanotubes were prepared by mixing aqueous solutions of the two porphyrins shown in Fig. 1 using a procedure slightly modified from that described previously² (see Experimental section).

The PNTs used in the Raman study are shown in a transmission electron microscope (TEM) image as an inset of Fig. 2. The hollow tubes, formed by ionic self-assembly of the porphyrins, are approximately 60 nm in diameter and can be up to several micrometres long. The ratio of 2.0–2.5 molecules of H₄TPPS₄²⁻ to 1.0 molecule of Sn(X)(X')TPyP^{4+/5+} [X, X' = OH⁻ or H₂O] is consistent with the ratio of the charges on the two porphyrins at pH 2.² The fact that the composition of the PNTs is

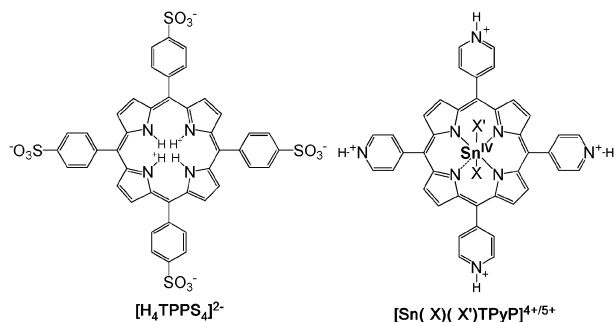


Fig. 1 Porphyrins used in the assembly of the porphyrin nanotubes depicted in the TEM image of Fig. 2. At pH 2, there is a mixture of Sn porphyrin complexes with X = OH⁻ and X' = H₂O (net charge +5) and X = X' = OH⁻ (net charge +4).²

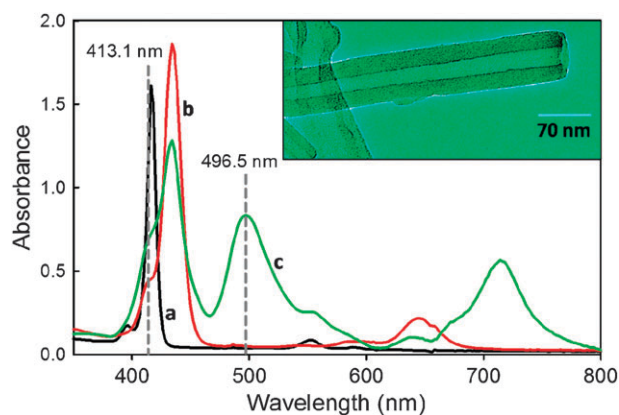


Fig. 2 UV-visible spectra of the porphyrin nanotubes and the constituent monomers at pH 2: SnTPyP^{4+/5+} (a); H₄TPPS₄²⁻ (b); and a colloidal suspension of the nanotubes (c). Dashed lines correspond to two of the laser excitation wavelengths used in the resonance Raman experiments (near the monomeric Soret region at 413.1 nm and near the *J*-aggregate band at 496.5 nm). Inset: TEM image of a PNT from the preparation used for the Raman spectra.

determined by the ionic interactions of the porphyrins confirms the formation of an ionic solid without additional counter ions. Other intermolecular interactions including van der Waals forces, hydrophobic interactions and hydrogen bonding also contribute to the formation and stability of the nanotubes.

B UV-visible spectroscopy

Fig. 2 shows the position of the laser excitation wavelengths relative to the absorption bands of the porphyrin nanotubes (Fig. 2, spectrum c) and the monomer-like Soret bands at 416 and 432 nm. These monomer-like bands of the nanotubes are at the same wavelengths as the Soret bands of SnTPyP^{4+/5+} (Fig. 2, spectrum a) and freshly prepared H₄TPPS₄²⁻ (Fig. 2, spectrum b). The monomer-like bands come from the nanotubes, not from dissolved porphyrin monomers in the supernatant, as they are also observed in the spectra of dry preparations of the nanotubes as films on glass slides. Red-shifted from these monomer-like bands of the tubes are two characteristic bands for porphyrin *J*-aggregates^{1,2} at 496 nm and 714 nm (Fig. 2, spectrum c). *J*-Aggregate bands also result from the coupling of transition dipoles of adjacent porphyrin molecules in H₄TPPS₄ self-aggregates.^{23–28} Given that there are two types of porphyrins present in the nanotubes, the origin of the exchange coupling emerges as a relevant question.

C Resonance Raman spectroscopy

In order to elucidate the electronic coupling between the porphyrins in the nanotubes, resonance Raman spectra of the porphyrin nanotubes (Fig. 3) were obtained with the 496.5 and 501.7 nm lines of an Ar⁺ laser for excitation near resonance with the *J*-aggregate band. In addition, spectra were obtained near resonance with the monomer-like Soret bands of the PNTs by using the 413.1 and 406.7 nm lines of a Kr⁺ laser. For comparison, spectra of the individual constituent porphyrins were also obtained at these wavelengths. Table 1 gives the frequencies of the Raman lines in the spectra taken at

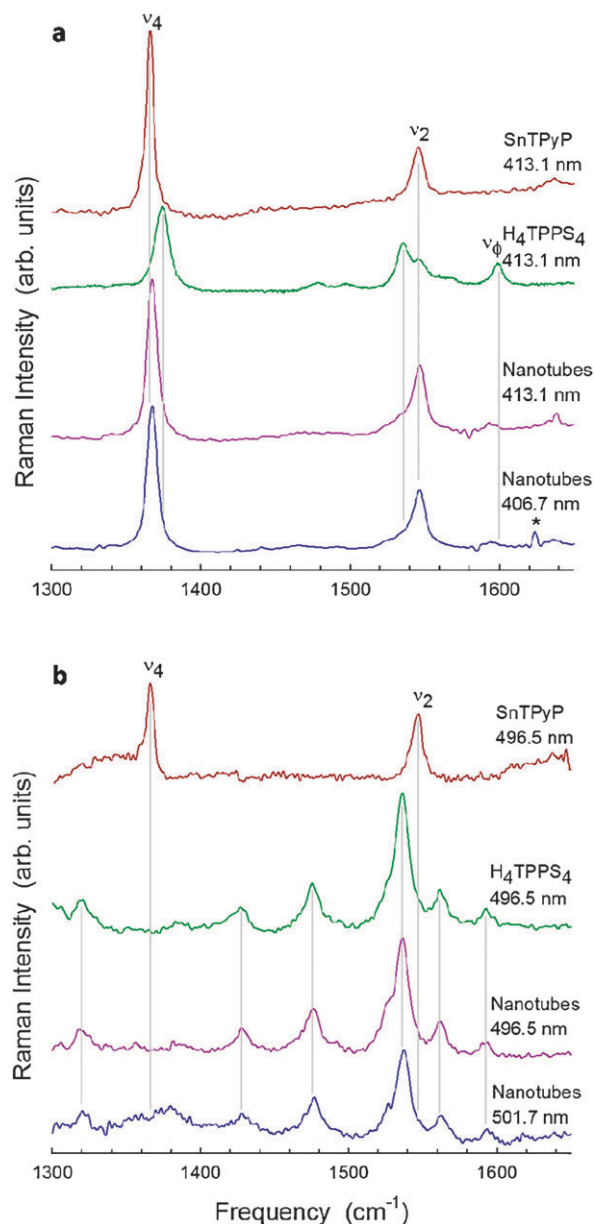


Fig. 3 Resonance Raman spectra of the porphyrin nanotubes (dark magenta, blue) and the individual porphyrins, H₄TPPS₄²⁻ (green) and SnTPyP^{4+/5+} (red) for: (a) laser excitation at the Soret region (413.1 and 406.7 nm) and (b) the *J*-aggregate band region (496.5 and 501.7 nm). Spectra of the individual porphyrins at 406.7 nm (a) and 501.7 nm (b) are not shown since they are very similar to those obtained at 413.1 nm and 496.5 nm, respectively. * indicates an emission line.

413.1 and 496.5 nm laser excitation wavelengths at resonance with the monomer-like and *J*-aggregate absorption bands, respectively.

Excitation at resonance with the monomer bands. Fig. 3a shows the resonance Raman spectra obtained with excitation near the monomer-like Soret bands of the nanotubes together with Raman data for the reference porphyrins. Excitation at 406.7 and 413.1 nm is close to the 0–0 Soret peak of monomeric SnTPyP and the 0–1 vibrational satellite of the Soret band of monomeric H₄TPPS₄ (Fig. 2a). Thus, resonance

Table 1 Frequencies (cm^{-1}) of the lines in the resonance Raman spectra of the monomeric porphyrins, the H_4TPPS_4 self-aggregate, and the porphyrin nanotubes at 413.1 and 496.5 nm excitation wavelengths

413.1 nm excitation			496.5 nm excitation			Assignment
SnTPyP	mono- H_4TPPS_4	Nanotubes	SnTPyP	agg- H_4TPPS_4	Nanotubes	
1636	—	1636	—	—	—	ν_{10}
—	1599	1594	—	1593	1592	$\nu_{\phi}(\text{C}=\text{C})$
—	1567	—	—	1561	1561	—
1546	1535	$\sim 1530,^a$ 1535, ^a 1547	1547	1536	1536	ν_2
—	1498	—	—	—	—	—
—	1477	—	—	1475	1475	ν_3
—	—	—	—	1427	1427	—
1365	1374	1366	1366	—	—	ν_4

^a Shoulder.

enhancement of the Raman lines of both monomeric porphyrins is expected and the lines observed for the individual porphyrins are the monomeric forms. Note, however, that the aged sample of H_4TPPS_4 used in the Raman studies is a mixture of monomeric and aggregated forms resulting from the well-known self-aggregation of $\text{H}_4\text{TPPS}_4^{2-}$. Under acidic conditions, self-aggregation of $\text{H}_4\text{TPPS}_4^{2-}$ can occur by neutralization of its two positive charges at the porphyrin core by the negative charges of the sulfonate groups at the periphery. Nevertheless, only the monomeric species is observed for Soret excitation.

For excitation near the monomer-like Soret bands of the nanotubes, the spectrum is clearly dominated by the lines of the Sn porphyrin, and the frequencies and relative intensities of the SnTPyP lines are virtually unchanged from the monomer spectra. The strongest lines of the nanotubes at 1366 and 1547 cm^{-1} in the 413.1 nm spectrum correspond to ν_4 and ν_2 of monomeric SnTPyP. The weak ν_{10} line of monomeric SnTPyP also appears at 1636 cm^{-1} in the porphyrin nanotube spectrum. These SnTPyP spectral features also appear in the spectrum of the nanotubes taken with 406.7 nm excitation. The frequencies of these lines of SnTPyP subunits of the nanotubes are thus very close to the frequencies obtained from monomeric SnTPyP (see Table 1).

The resonance Raman lines of the H_4TPPS_4 species are also in evidence in the Soret resonance spectra, and the frequencies are generally in good agreement with previous Raman studies of H_4TPPS_4 self-aggregates.^{26,29} Lines attributable to the H_4TPPS_4 subunits of the nanotubes are evident, primarily in the appearance of the phenyl line (ν_{ϕ}) at 1594 cm^{-1} downshifted from the true monomer frequency of 1599 cm^{-1} . Contributions from other lines of H_4TPPS_4 appear as shoulders on the strong Sn-porphyrin lines (Fig. 3a). Specifically, H_4TPPS_4 is evident in the increased intensity on the high frequency side of ν_4 of the Sn porphyrin and the unresolved shoulder on the low frequency side of ν_2 of SnTPyP at 1535 cm^{-1} . Weaker lines of the H_4TPPS_4 are not obviously observed in the spectrum of the nanotubes taken with 413.1 nm excitation. As expected, the H_4TPPS_4 contributions to the PNT spectrum subtly decrease in intensity when the resonance condition for the Soret bands changes with excitation at 406.7 nm (bottom spectrum in Fig. 3a).

The frequencies of lines for H_4TPPS_4 (e.g., ν_{ϕ}) in the PNTs at 413.1 nm excitation are altered from the monomer values (see Table 1). The frequencies for the PNTs are consistent with the

formation of H_4TPPS_4 aggregates.^{26,29} That is, agg- H_4TPPS_4 frequencies are found for the nanotubes even for resonance with the monomer-like absorption bands of the PNTs. In contrast, Soret excitation of the H_4TPPS_4 solution gives the true monomer spectrum (mono- H_4TPPS_4). Apparently, there is very little monomer-like H_4TPPS_4 present in the nanotubes, but the H_4TPPS_4 solution contains enough monomer so that it dominates the Raman spectra taken at resonance with the Soret band.

Excitation at resonance with the *J*-aggregate band. Raman spectra obtained with laser wavelengths at resonance with the *J*-aggregate band of the nanotubes provide insight into the porphyrin organization and electronic coupling between molecules within the nanostructure. Unexpectedly, resonance Raman spectra of the nanotubes obtained at 496.5 or 501.7 nm excitation (Fig. 3b) shows only the aggregated form of H_4TPPS_4 . The PNT spectrum is almost identical to the spectra of H_4TPPS_4 self-aggregates^{26,29,30} taken at 496.5 nm, for which the fraction of H_4TPPS_4 that is aggregated at the acidic pH of the experiment satisfies the resonance condition and is preferentially enhanced. This suggests that there is some similarity between the H_4TPPS_4 aggregation motif in the nanotubes and that of the H_4TPPS_4 self-aggregates.

Remarkably, the strong ν_4 and ν_2 lines of SnTPyP are not found in the nanotube spectra. H_4TPPS_4 is present in only a 2-fold excess over the Sn porphyrin, so we would still expect to see the strongest Raman lines of SnTPyP if they were enhanced.

IV. Discussion

Taken together, the resonance Raman results indicate that the Sn porphyrins do not form *J*-aggregates within the tubes. If the Sn porphyrin were in *J*-aggregates this should be evident in the spectra obtained at resonance with the *J*-aggregate band, but no Raman lines from the Sn porphyrin are observed. The Raman data also indicate that H_4TPPS_4 forms *J*-aggregates in the PNTs that are segregated from the SnTPyP molecules. Thus, SnTPyP molecules do not participate in the H_4TPPS_4 *J*-aggregates nor do they form separate *J*-aggregates with a UV-visible band near 500 nm.

H_4TPPS_4 is known to form *J*-aggregates in the form of monolayer-thick tubes under acidic (pH 1) solution conditions.^{27,29} H_4TPPS_4 apparently also forms similar *J*-aggregates within the binary PNT. Segregation of the two porphyrins within the tube structure might occur for several reasons including the

disparity of charges present on the porphyrins and consequent amounts of the two porphyrins in the tubes. Specifically, the higher charge on SnTPyP^{4+/5+} and hence lower abundance in the tubes implies it must interact with several adjacent molecules of H₄TPPS₄ to obtain local charge neutrality. For this reason, the slipped stacking of the typical *J*-aggregate is less likely to occur because the SnTPyP molecules must be more dispersed in the solid. In addition, the obligate axial ligands (H₂O, OH⁻) of the Sn(IV) porphyrin is expected to inhibit the porphyrin macrocycle stacking^{31–34} and formation of *J*-aggregates.

The formation of a binary structure with Sn porphyrin molecules does alter the structure of the H₄TPPS₄ aggregates in the nanotubes *versus* H₄TPPS₄ self-aggregates. Specifically, the UV-visible absorption spectrum of the nanotubes indicates shortening of the coherence length for the coupling of transition dipoles in the H₄TPPS₄ stacks. For H₄TPPS₄ self-aggregates that form at low pH and high ionic strength, it is estimated that transition dipoles of the molecules are exchange coupled over 14 to 16 adjacent molecules in H₄TPPS₄ slipped stacks,^{25,29} giving rise to a very exchange-narrowed *J*-aggregate band.^{27,28} Based on the broader *J*-aggregate UV-visible bands of the nanotubes (Fig. 2) in comparison with the H₄TPPS₄ *J*-aggregate bands, the coupling must extend over fewer molecules than for the self-aggregates. This could be the result of Sn porphyrin molecules being interspersed within the H₄TPPS₄ slipped face-to-face stacks, thereby interrupting the usual dipolar couplings that give rise to the *J*-aggregate bands. In this regard, it is possible that two Sn porphyrins initially form neutral hexamers or heptamers with 4 or 5 H₄TPPS₄ molecules, with the SnTPyP^{4+/5+} molecules terminating the dipole coupling. The initial formation of these neutral subunits would largely neutralize the strong electrostatic interactions between the porphyrin tectons, and subsequently, these putative neutral subunits could self-assemble into the nanotubes. A similar subunit assembly mechanism has been proposed for H₄TPPS₄ self-aggregates.²⁹ Another attractive mechanism for the formation of the PNTs is the formation of a nucleating monolayer tube of H₄TPPS₄ followed by a disperse layer of SnTPyP molecules. Successive alternating monolayers of slip-stacked H₄TPPS₄ and more thinly spread SnTPyP would explain the concentric fringes seen in the end-on TEM images of the porphyrin nanotubes.²

V. Conclusions

The precise structure of H₄TPPS₄²⁻ homo-aggregates has been the source of considerable debate. Recent structural and spectroscopic studies strongly support the idea that H₄TPPS₄²⁻ forms monolayer thick nanotubes,^{27–29} although there is still no consensus on the structure of the monolayer (rolled sheets²⁸ *versus* disk-like building blocks²⁹). Significantly, the internal arrangement of the porphyrin molecules in the ionically self-assembled porphyrin nanotubes discussed here must be more complex than for the monolayer nanotubes of the H₄TPPS₄ self-aggregates. Specifically, the H₄TPPS₄ component segregates and forms *J*-aggregates, while the other porphyrins (SnTPyP^{4+/5+}) serve as counter ions without forming separate *J*-aggregate stacks. In other words, the

resonance Raman spectra indicate a segregated packing arrangement of the two porphyrin components in the tubes. The lamellar structure² of the nanotubes seen in TEM images of the nanotubes trapped in end-on orientations may also indicate that the nanotubes are composed of layers of H₄TPPS₄, similar to the monolayer thick nanotubes of H₄TPPS₄ observed in cryo-TEM studies of frozen suspensions,²⁸ alternating with layers of SnTPyP acting as counter ions. Resonance Raman spectroscopy provides a useful probe of the molecular organization in the absence of detailed X-ray structural information, which is often not attainable for nanoscale structures. Regardless of the exact molecular organization, these nanotubes possess a unique internal structure that may lead to novel optomechanical, photophysical, and photochemical properties. In this regard, the delocalization of excitons in the porphyrin nanotubes points to high exciton mobilities, which are desirable for applications in areas such as light-harvesting in solar energy systems, sensors, and electronics.

Acknowledgements

Sandia is a multiprogram laboratory operated by Sandia Corporation, a Lockheed Martin Company, for the United States Department of Energy's National Nuclear Security Administration under Contract DEAC04-94AL85000. Research supported by the Laboratory Directed Research and Development program at Sandia National Laboratories and the U.S. Department of Energy, Office of Basic Energy Sciences, Division of Materials Sciences and Engineering. FLAD (Luso-American Foundation, Portugal) is gratefully acknowledged for financial support of this work.

References

- 1 X. W. Li, Z. L. Zheng, M. Y. Han, Z. P. Chen and G. L. Zou, *J. Phys. Chem. B*, 2007, **111**, 4342.
- 2 Z. C. Wang, C. J. Medforth and J. A. Shelnutt, *J. Am. Chem. Soc.*, 2004, **126**, 15954.
- 3 C. J. Medforth, Z. Wang, K. E. Martin, Y. Song, J. L. Jacobsen and J. A. Shelnutt, *Chem. Commun.*, 2009, 7261.
- 4 P. E. Burrows, S. R. Forrest, S. P. Sibley and M. E. Thompson, *Appl. Phys. Lett.*, 1996, **69**, 2959.
- 5 C. Y. Liu, H. I. Pan, M. A. Fox and A. J. Bard, *Science*, 1993, **261**, 897.
- 6 T. Malinski and Z. Taha, *Nature*, 1992, **358**, 676.
- 7 C. H. M. Marée, S. J. Roosendaal, T. J. Savenije, R. E. I. Schropp, T. J. Schaafsma and F. H. P. M. Habraken, *J. Appl. Phys.*, 1996, **80**, 3381.
- 8 T. Hasobe, H. Oki, A. S. D. Sandanayaka and H. Murata, *Chem. Commun.*, 2008, 724.
- 9 Z. Wang, L. E. Lybarger, W. Wang, C. J. Medforth, J. E. Miller and J. A. Shelnutt, *Nanotechnology*, 2008, **19**, 395604.
- 10 B. Ventura, F. Barigelletti, F. Lodato, D. L. Officer and L. Flamigni, *Phys. Chem. Chem. Phys.*, 2009, **11**, 2166.
- 11 M. J. Ahrens, R. F. Kelley, Z. E. X. Dance and M. R. Wasielewski, *Phys. Chem. Chem. Phys.*, 2007, **9**, 1469.
- 12 T. Jochum, C. M. Reddy, A. Eichhöfer, G. Buth, J. Szymkowski, H. Kalt, D. Moss and T. S. Balaban, *Proc. Natl. Acad. Sci. U. S. A.*, 2008, **105**, 12736.
- 13 S. Ganapathy, G. T. Oostergetel, P. K. Wawrzyniak, M. Reus, A. Gomez Maqueo Chew, F. Buda, E. J. Boekema, D. A. Bryant, A. R. Holzwarth and H. J. M. de Groot, *Proc. Natl. Acad. Sci. U. S. A.*, 2009, **106**, 8525.
- 14 T. Kojima, R. Harada, T. Nakanishi, K. Kaneko and S. Fukuzumi, *Chem. Mater.*, 2007, **19**, 51.

-
- 15 Z. Wang, K. J. Ho, C. J. Medforth and J. A. Shelnut, *Adv. Mater.*, 2006, **18**, 2557.
 - 16 J. H. Jang, K. S. Jeon, S. Oh, H. J. Kim, T. Asahi, H. Masuhara and M. Yoon, *Chem. Mater.*, 2007, **19**, 1984.
 - 17 K. Akatsuka, Y. Ebina, M. Muramatsu, T. Sato, H. Hester, D. Kumaresan, R. H. Schmehl, T. Sasaki and M. A. Haga, *Langmuir*, 2007, **23**, 6730.
 - 18 Z. C. Wang, Z. Y. Li, C. J. Medforth and J. A. Shelnut, *J. Am. Chem. Soc.*, 2007, **129**, 2440.
 - 19 Y. Kim, M. F. Mayer and S. C. Zimmerman, *Angew. Chem., Int. Ed.*, 2003, **42**, 1121.
 - 20 T. Yamaguchi, N. Ishii, K. Tashiro and T. Aida, *J. Am. Chem. Soc.*, 2003, **125**, 13934.
 - 21 K. Hosomizu, M. Odoi, T. Umeyama, Y. Matano, K. Yoshida, S. Isoda, M. Isosomppi, N. V. Tkachenko, H. Lemmetyinen and H. Imahori, *J. Phys. Chem. B*, 2008, **112**, 16517.
 - 22 Z. C. Wang, C. J. Medforth and J. A. Shelnut, *J. Am. Chem. Soc.*, 2004, **126**, 16720.
 - 23 E. B. Fleischer, J. M. Palmer, T. S. Srivastava and A. Chatterjee, *J. Am. Chem. Soc.*, 1971, **93**, 3162.
 - 24 R. F. Pasternack, P. R. Huber, P. Boyd, G. Engasser, L. Francesconi, E. Gibbs, P. Fasella, G. C. Venturo and L. de C. Hinds, *J. Am. Chem. Soc.*, 1972, **94**, 4511.
 - 25 A. S. R. Koti, J. Taneja and N. Periasamy, *Chem. Phys. Lett.*, 2003, **375**, 171.
 - 26 O. Ohno, Y. Kaizu and H. Kobayashi, *J. Chem. Phys.*, 1993, **99**, 4128.
 - 27 A. D. Schwab, D. E. Smith, C. S. Rich, E. R. Young, W. F. Smith and J. C. de Paula, *J. Phys. Chem. B*, 2003, **107**, 11339.
 - 28 S. M. Vlaming, R. Augulis, M. C. A. Stuart, J. Knoester and P. H. M. van Loosdrecht, *J. Phys. Chem. B*, 2009, **113**, 2273.
 - 29 B. A. Friesen, K. R. A. Nishida, J. L. McHale and U. Mazur, *J. Phys. Chem. C*, 2009, **113**, 1709.
 - 30 D.-M. Chen, T. He, D.-F. Cong, Y.-H. Zhang and F.-C. Liu, *J. Phys. Chem. A*, 2001, **105**, 3981.
 - 31 J. A. Shelnut, *Inorg. Chem.*, 1983, **22**, 2535.
 - 32 J. A. Shelnut, M. M. Dobry and J. D. Satterlee, *J. Phys. Chem.*, 1984, **88**, 4980.
 - 33 J. A. Shelnut, *J. Am. Chem. Soc.*, 1981, **103**, 4275.
 - 34 J. A. Shelnut, *J. Am. Chem. Soc.*, 1983, **105**, 7179.